Growth and Remodelling of Intracranial Saccular Aneurysms

Antonio DiCarlo[1], Vittorio Sansalone[2], Amabile Tatone[3], and Valerio Varano[1]

[1]LaMS – Modelling & Simulation Lab, Università Roma Tre, Italy,
[2]Laboratoire de Mécanique Physique, Université Paris Est, France,
[3]DISAT, Università degli Studi dell'Aquila, Italy.

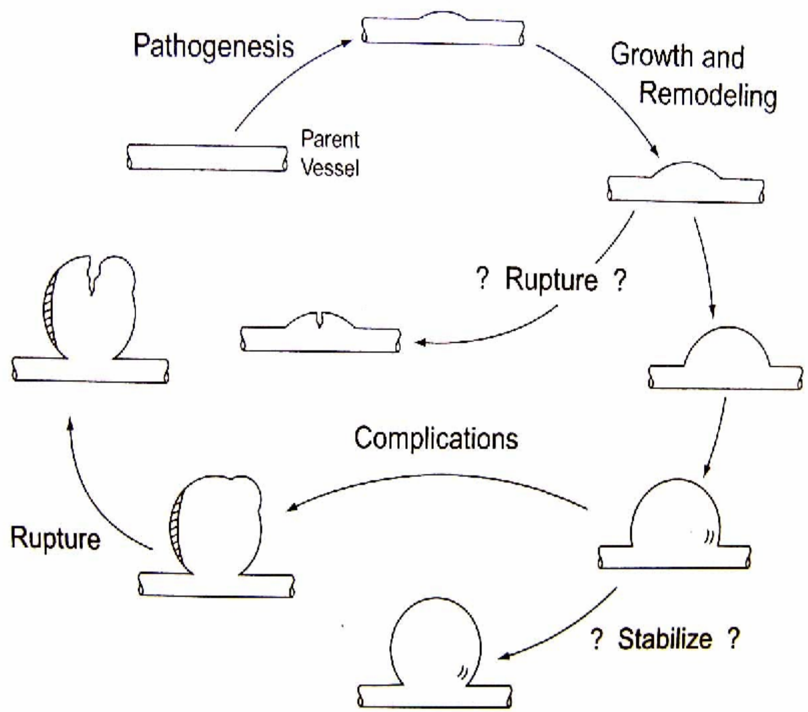
Pathogenesis
Growth and Remodeling
Parent Vessel
? Rupture ?
Complications
Rupture
? Stabilize ?

Spherical symmetry

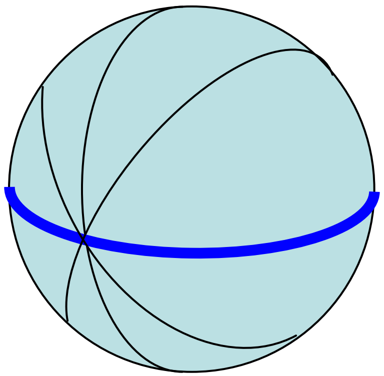

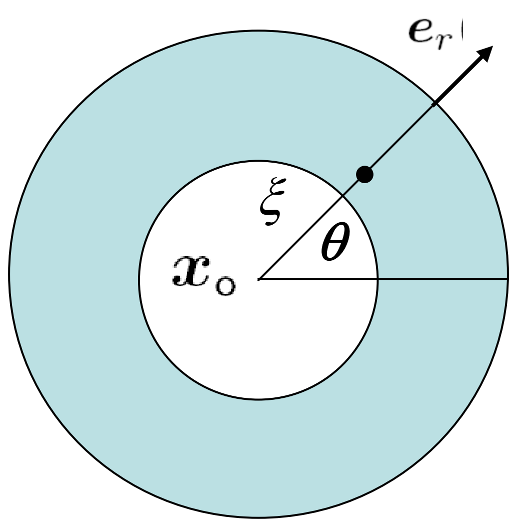

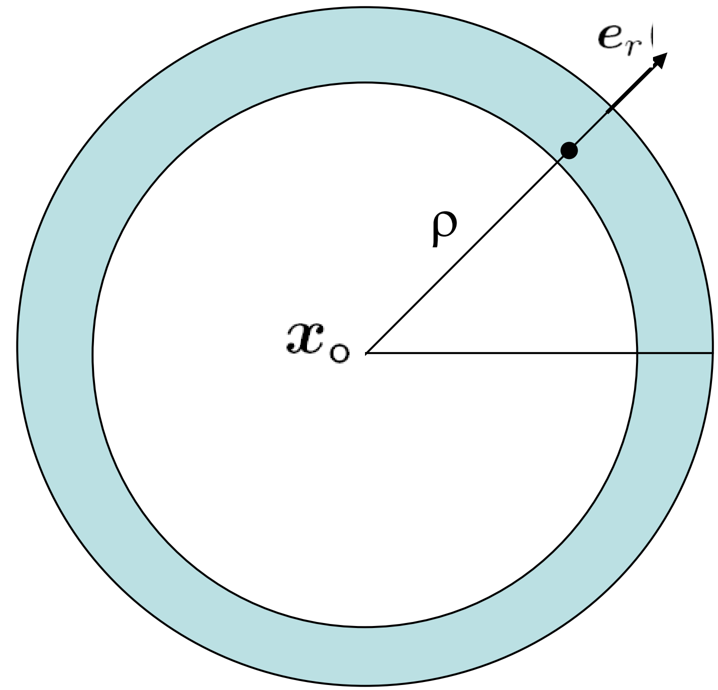

$$\mathsf{p}(\boldsymbol{x},\tau) \;=\; \boldsymbol{x}_\circ + \rho\,(\xi,\tau)\,\boldsymbol{e}_r(\vartheta,\varphi)$$

$$\nabla\mathsf{p}(\boldsymbol{x},\tau) = \rho'(\xi,\tau)\,\mathbf{P}_r(\vartheta,\varphi) + \frac{\rho}{\xi}(\xi,\tau)\,\mathbf{P}_h(\vartheta,\varphi)$$

$$\mathbf{P}_r := \boldsymbol{e}_r \otimes \boldsymbol{e}_r,\; \mathbf{P}_h := \mathbf{I} - \mathbf{P}_r$$

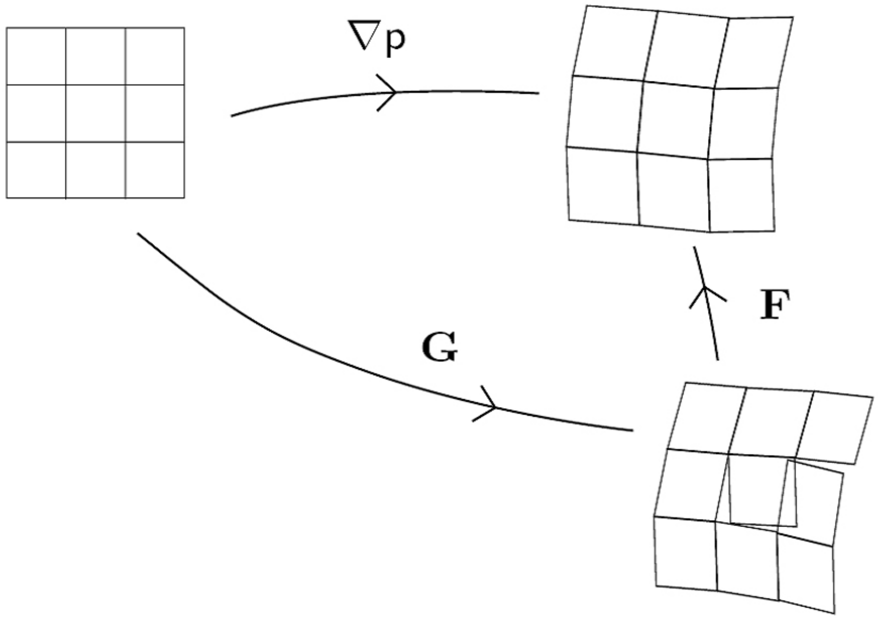

Kröner-Lee decomposition

$$\mathbf{G} : (\boldsymbol{x}, \tau) \mapsto \gamma_r(\xi, \tau)\, \mathbf{P}_r(\vartheta, \varphi) + \gamma_h(\xi, \tau)\, \mathbf{P}_h(\vartheta, \varphi)$$

$$\mathbf{F} := \nabla \mathsf{p} \mathbf{G}^{-1} = \lambda_r\, \mathbf{P}_r + \lambda_h\, \mathbf{P}_h \qquad \lambda_r := \frac{\rho'}{\gamma_r}\,, \qquad \lambda_h := \frac{\rho}{\xi\, \gamma_h}$$

$$J(\boldsymbol{x}, \tau) := \det \mathbf{G}(\boldsymbol{x}, \tau) = \gamma_r(\xi, \tau)\, \gamma_h(\xi, \tau)^2$$

COMSOL CONFERENCE MILAN 2009

Multiple remodeling mechanisms

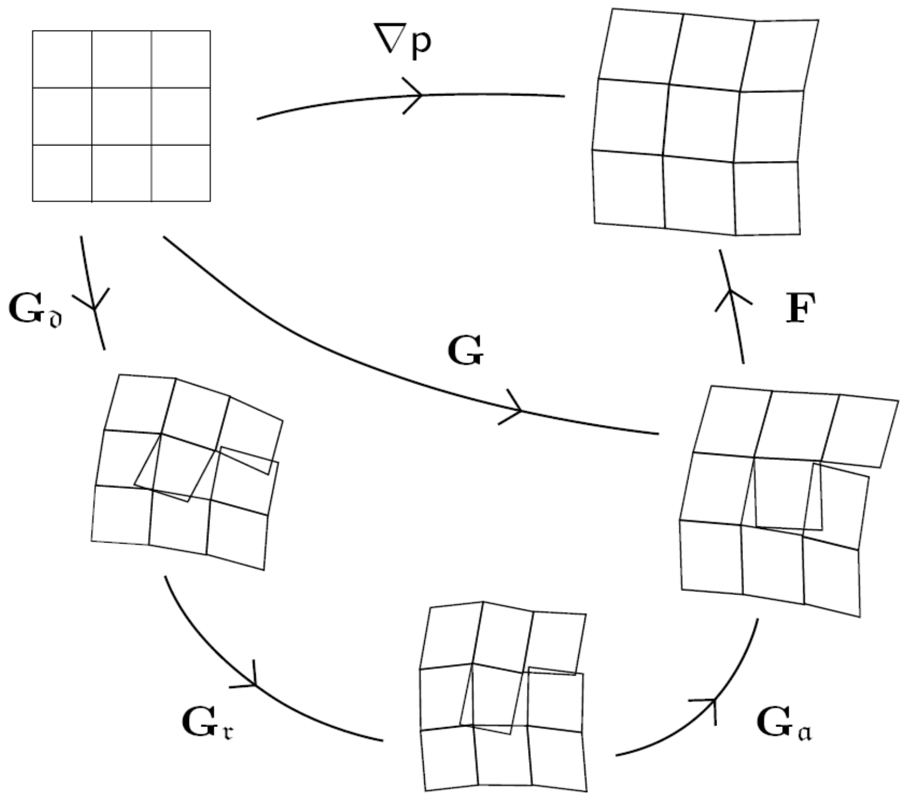

$$\mathbf{G} = \mathbf{G}_{\mathfrak{a}}\,\mathbf{G}_{\mathfrak{r}}\,\mathbf{G}_{\mathfrak{d}}$$

COMSOL CONFERENCE MILAN 2009

Multiple remodeling mechanisms

$$J_{\mathfrak{d}} := \det \mathbf{G}_{\mathfrak{d}} = 1 \quad \Leftrightarrow \quad \mathbf{G}_{\mathfrak{d}} = \gamma_{\mathfrak{d}}^{-2}\,\mathbf{P}_r + \gamma_{\mathfrak{d}}\,\mathbf{P}_h$$ Decay — passive

$$J_{\mathfrak{r}} := \det \mathbf{G}_{\mathfrak{r}} = 1 \quad \Leftrightarrow \quad \mathbf{G}_{\mathfrak{r}} = \gamma_{\mathfrak{r}}^{-2}\,\mathbf{P}_r + \gamma_{\mathfrak{r}}\,\mathbf{P}_h$$ Recovery

$$\mathbf{G}_{\mathfrak{a}} = \gamma_{\mathfrak{a}}\,\mathbf{P}_r + \mathbf{P}_h \quad \Rightarrow \quad \mathbf{G}_{\mathfrak{a}} = \gamma_{\mathfrak{a}}\,\mathbf{P}_r + \mathbf{P}_h$$ Apposition

(Recovery and Apposition: active)

$$\Rightarrow$$

$$\mathbf{G} = \gamma_{\mathfrak{a}}(\gamma_{\mathfrak{d}}\gamma_{\mathfrak{r}})^{-2}\,\mathbf{P}_r + \gamma_{\mathfrak{d}}\gamma_{\mathfrak{r}}\,\mathbf{P}_h$$

COMSOL CONFERENCE 2009 MILAN

Virtual Work

$$\int_{\mathscr{D}} (-\mathbf{S} \cdot \nabla \boldsymbol{v}) + \int_{\partial \mathscr{D}} \boldsymbol{t}_{\partial \mathscr{D}} \cdot \boldsymbol{v} + \int_{\mathscr{D}} J(\mathbb{A}_{\mathfrak{d}} \cdot \mathbf{V}_{\mathfrak{d}} + \mathbb{A}_{\mathfrak{r}} \cdot \mathbf{V}_{\mathfrak{r}} + \mathbb{A}_{\mathfrak{a}} \cdot \mathbf{V}_{\mathfrak{a}})$$

Balance equations

$$2\left(\mathrm{S}_r(\xi) - \mathrm{S}_h(\xi)\right) + \xi\, \mathrm{S}'_r(\xi) = 0\,,$$

$$\mathcal{A}_{\mathfrak{d}} = \mathcal{A}^{\mathfrak{i}}_{\mathfrak{d}} + \mathcal{A}^{\mathfrak{o}}_{\mathfrak{d}} = 0\,,$$
$$\mathcal{A}_{\mathfrak{r}} = \mathcal{A}^{\mathfrak{i}}_{\mathfrak{r}} + \mathcal{A}^{\mathfrak{o}}_{\mathfrak{r}} = 0\,,$$
$$\mathcal{A}_{\mathfrak{a}} = \mathcal{A}^{\mathfrak{i}}_{\mathfrak{a}} + \mathcal{A}^{\mathfrak{o}}_{\mathfrak{a}} = 0\,,$$

for all $\xi_- < \xi < \xi_+$, and

$$\mathrm{S}_r(\xi_\mp) = -\pi_\mp\,,$$

COMSOL CONFERENCE MILAN 2009

Dissipative inner actions

$$\overset{+}{\mathcal{A}}_{\mathfrak{d}} = -\, d_{\mathfrak{d}}\, \frac{\dot{\gamma}_{\mathfrak{d}}}{\gamma_{\mathfrak{d}}}\,,\; \overset{+}{\mathcal{A}}_{\mathfrak{r}} = -\, d_{\mathfrak{r}}\, \frac{\dot{\gamma}_{\mathfrak{r}}}{\gamma_{\mathfrak{r}}}\,,\; \overset{+}{\mathcal{A}}_{\mathfrak{a}} = -\, d_{\mathfrak{a}}\, \frac{\dot{\gamma}_{\mathfrak{a}}}{\gamma_{\mathfrak{d}}}$$

Outer actions

$$\mathcal{A}^{\mathfrak{o}}_{\mathfrak{d}}(\xi,\tau) = 0\,,$$

$$\mathcal{A}^{\mathfrak{o}}_{\mathfrak{r}}(\xi,\tau) = \widehat{\mathcal{A}}_{\mathfrak{r}}\big(\mathbf{T}(\xi,\tau), \mathbf{T}^{\diamond}(\xi,\tau), \tau\big)$$

$$\mathcal{A}^{\mathfrak{o}}_{\mathfrak{a}}(\xi,\tau) = \widehat{\mathcal{A}}_{\mathfrak{a}}\big(\mathbf{T}(\xi,\tau), \mathbf{T}^{\diamond}(\xi,\tau), \tau\big)$$

Controls

$$\widehat{\mathcal{A}}_{\mathfrak{r}}\big(\mathbf{T}, \mathbf{T}^{\diamond}\big) = -\mathrm{E}_{\mathfrak{d}\&\mathfrak{r}}(\mathbf{T}) - f_{\mathfrak{r}}\,(\mathrm{T}_h - \mathrm{T}_h^{\diamond}) + c_{\mathfrak{r}}\,\frac{\rho - \bar{\rho}}{\rho'}\,(\mathrm{T}_h - \mathrm{T}_h^{\diamond})'$$

$$\widehat{\mathcal{A}}_{\mathfrak{a}}\big(\mathbf{T}, \mathbf{T}^{\diamond}\big) = -\mathrm{E}_{\mathfrak{a}}(\mathbf{T}) + f_{\mathfrak{a}}\,(\mathrm{T}_h - \mathrm{T}_h^{\diamond})$$

COMSOL CONFERENCE MILAN 2009

Balance equation

$$2\left(\mathrm{S}_r(\xi)-\mathrm{S}_h(\xi)\right)+\xi\,\mathrm{S}_r'(\xi)=0\,;$$

Evolution equations

$$\frac{\dot{\gamma}_h}{\gamma_h}=\frac{\mu_{\mathfrak{r}}}{d_{\mathfrak{d}}}\Big(\mathrm{E}_{\mathfrak{d}\&\mathfrak{r}}(\mathbf{T})+\widehat{\mathcal{A}}_{\mathfrak{r}}(\mathbf{T},\mathbf{T}^{\diamond})\Big),$$

$$\frac{\dot{\gamma}_r}{\gamma_r}+2\,\frac{\dot{\gamma}_h}{\gamma_h}=\frac{\mu_{\mathfrak{a}}}{d_{\mathfrak{d}}}\Big(\mathrm{E}_{\mathfrak{a}}(\mathbf{T})+\widehat{\mathcal{A}}_{\mathfrak{a}}(\mathbf{T},\mathbf{T}^{\diamond})\Big)$$

Use of COMSOL Script

Param_Values	Input parameters values
do_fem0	Homeostatic initial solution. weak form **femnlin** solver
do_fem1	Time dependent solution. weak form **femtime** solver
do_plot_t	Time plots
do_plot_f	Fields plots

Recovery control-I

$$f_{\mathfrak{a}} = 0,\ f_{\mathfrak{r}} > 0 \text{ and } c_{\mathfrak{r}} = 0$$

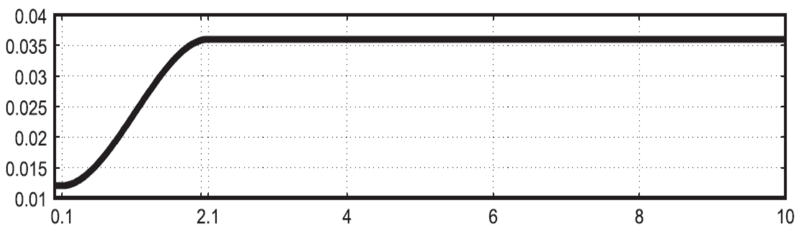

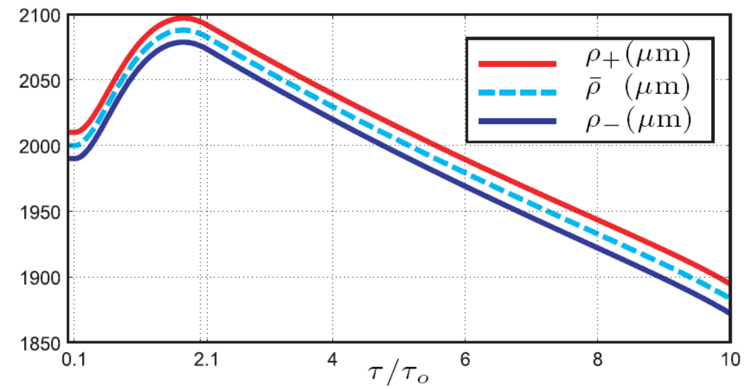

Figure 2: Actual radius vs time.

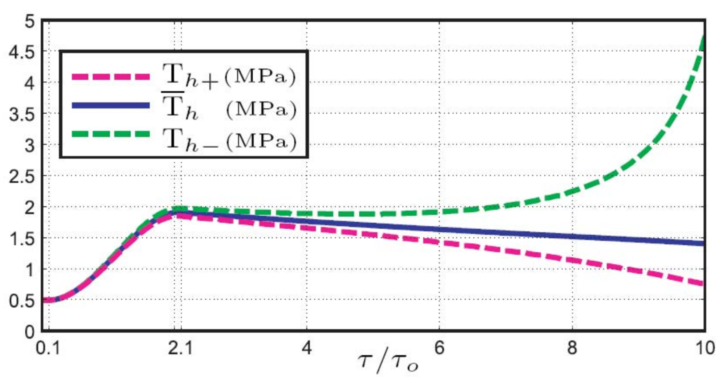

Figure 3: Hoop stress vs time.

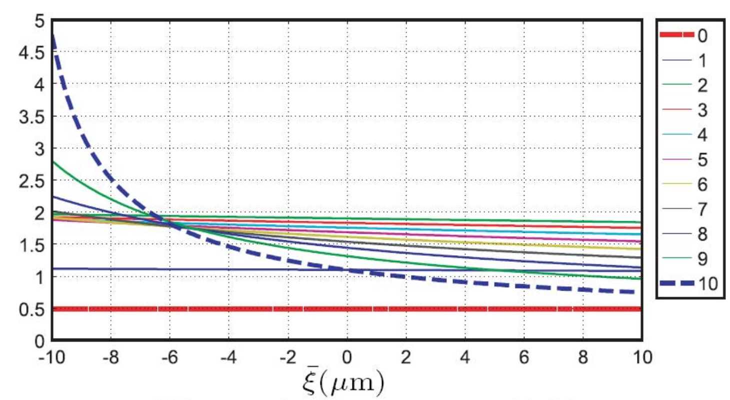

Figure 4: Hoop stress field.

Recovery control-II

$$f_{\mathfrak{a}} = 0,\ f_{\mathfrak{r}} > 0 \ \text{and} \ c_{\mathfrak{r}} > 0$$

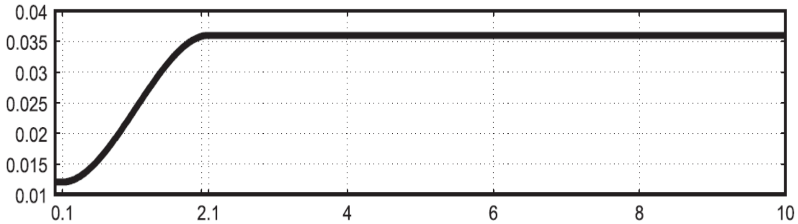

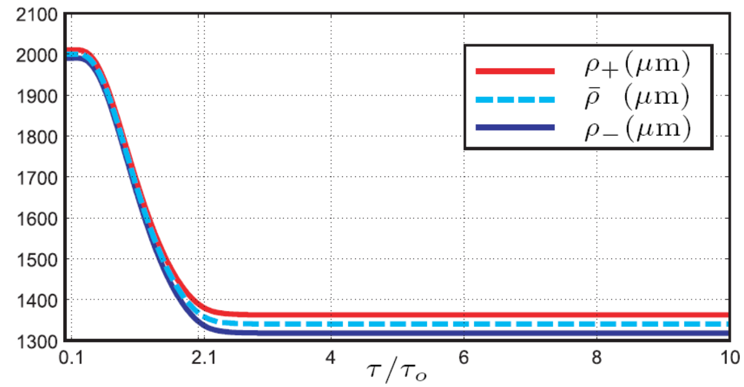

Figure 5: Actual radius vs time.

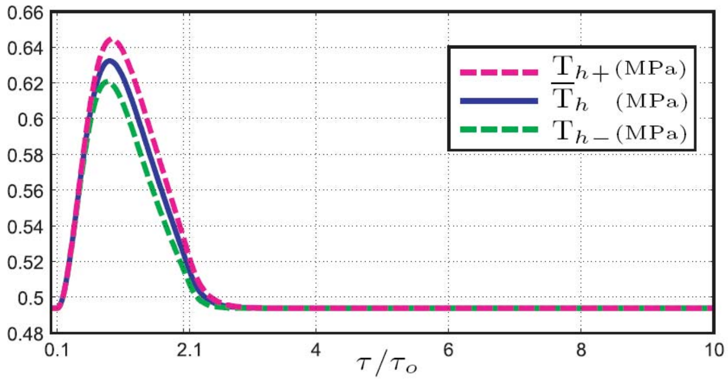

Figure 6: Hoop stress vs time.

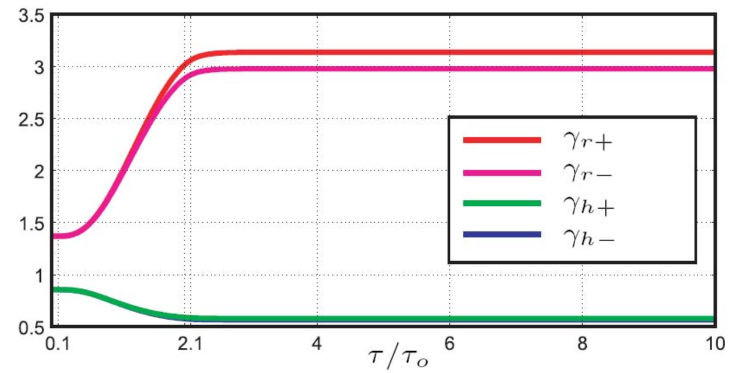

Figure 7: Transformation stretches vs time.

Apposition control

$$f_{\mathfrak{a}} > 0,\ f_{\mathfrak{r}} = 0 \text{ and } c_{\mathfrak{r}} = 0$$

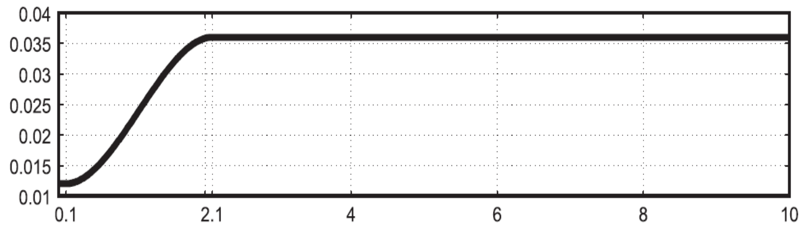

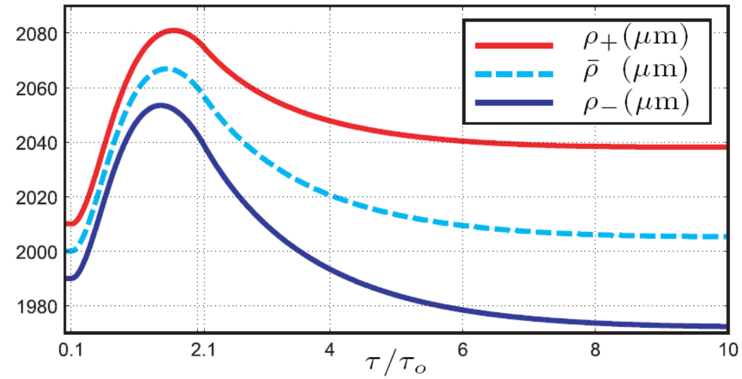

Figure 8: Actual radius vs time.

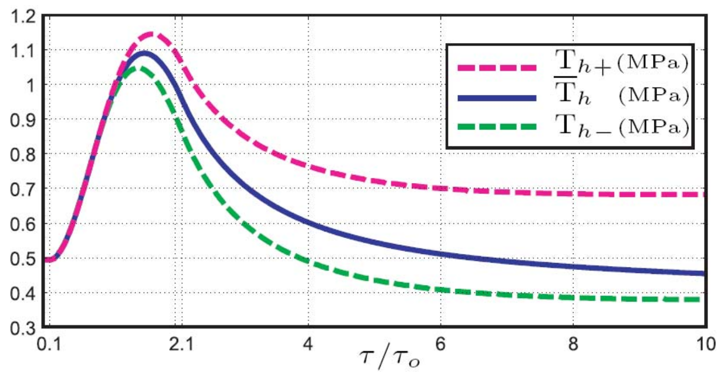

Figure 9: Hoop stress vs time.

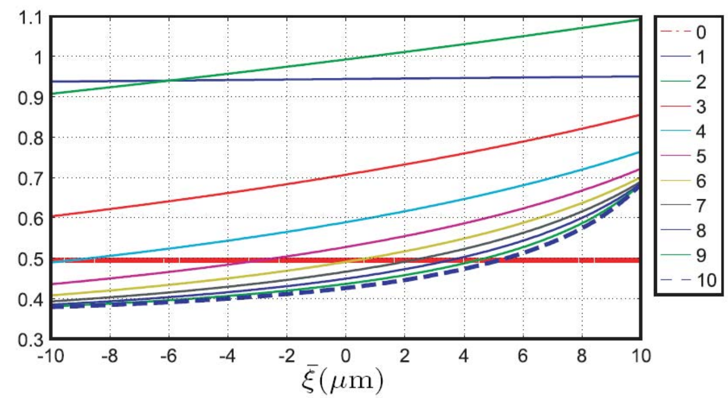

Figure 10: Hoop stress field.

Mixed control

$f_{\mathfrak{a}} > 0,\ f_{\mathfrak{r}} = 0 \text{ and } c_{\mathfrak{r}} > 0$

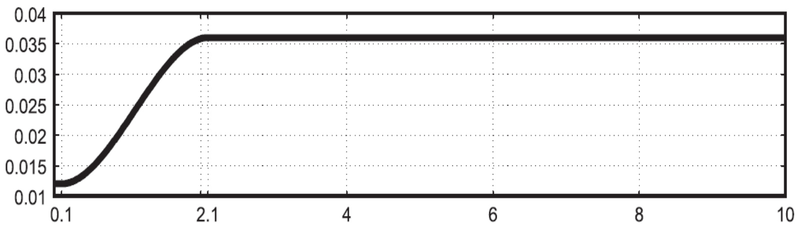

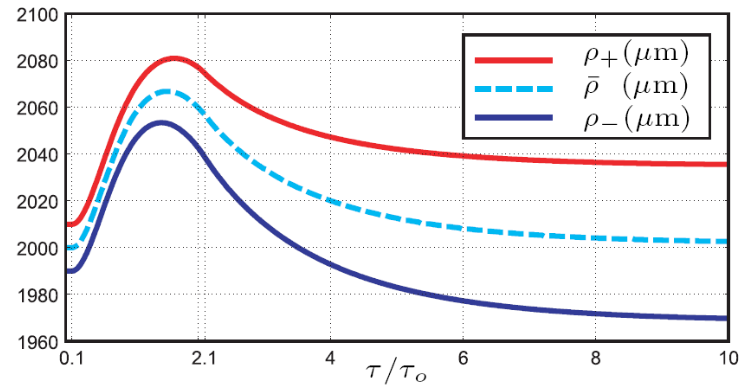

Figure 11: Actual radius vs time.

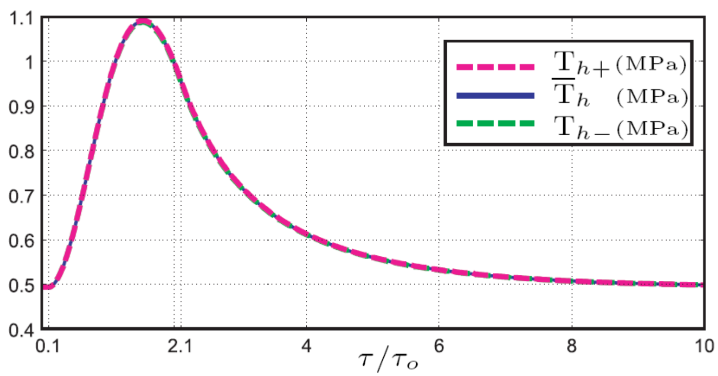

Figure 12: Hoop stress vs time.

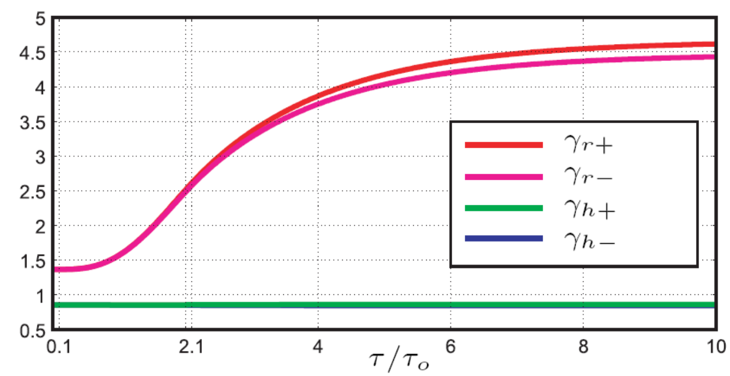

Figure 13: Transformation stretches vs time.

Conclusion

We have proposed a mechanical model—a growing spherical shell—suitable for predicting the evolution of a Saccular Cerebral Artery Aneurysms (SCAA), based on three competing remodeling mechanisms—one passive and two active. Despite drastic simplifying assumptions, preliminary numerical experiments attest to the potential of our model to account for nontrivial evolutions ensuing from accidental perturbations of a homeostatic state.

References

[1] A. DiCarlo and S. Quiligotti, *Growth and balance*, Mechanics Research Communications **29** (2002), no. 6, 449–456.

[2] J.D. Humphrey, *Cardiovascular solid mechanics: Cells, tissues, and organs*, Springer, New York, NY, 2001.

[3] S.K. Kyriacou and J.D. Humphrey, *Influence of size, shape and properties on the mechanics of axisymmetric saccular aneurysms*, Journal of Biomechanics **29** (1996), no. 8, 1015–1022, erratum 30: 761, 1997.